Forbush Decrease

封莉 紫金山天文台
郭静楠、Johan von Forstner 德国基尔大学
顾斌、倪素兰 南京信息工程大学

Outline

1. Solar modulation of cosmic ray intensity

2. Forbush decrease
   - ◆introduction to CME and its driven shock, and the related Forbush decrease
   - ◆Observational analyses
   - ◆FD simulations
   - ◆FD prediction

3. Sun shadow & CME shadow

   magnetic field modeling from line-of-sight and vector photosphere magnetic field

   MHD simulation: e.g. ENLIL model, NSSC COIN-TVD model

Solar modulation

Solar cycle: 11/22 years
Solar rotation: 27 days
Earth rotation: diurnal

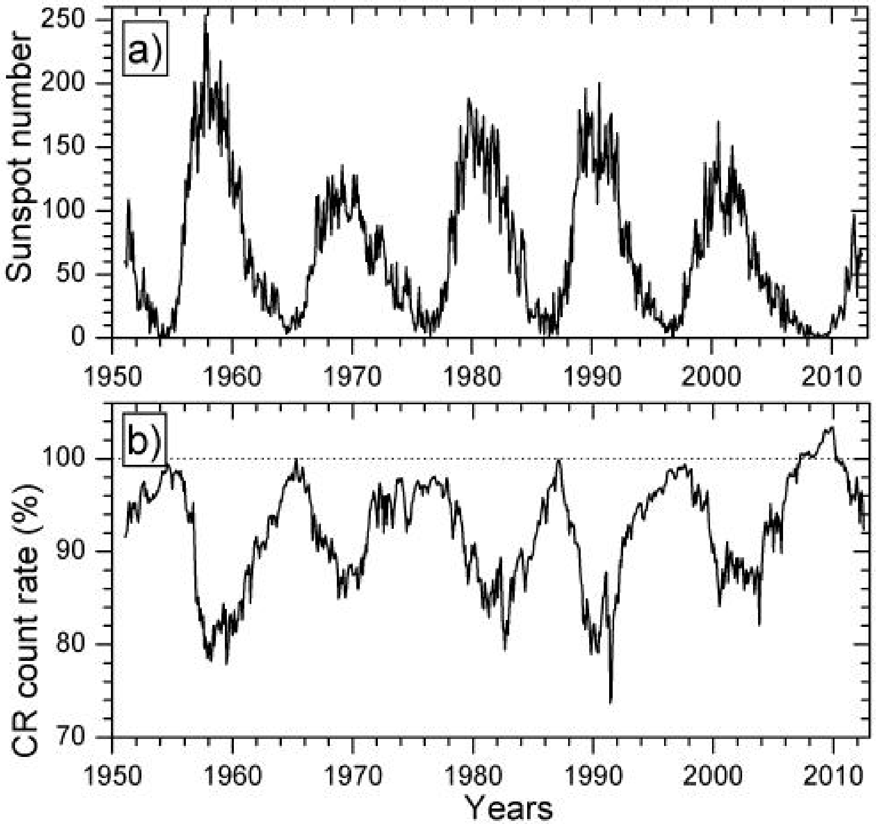

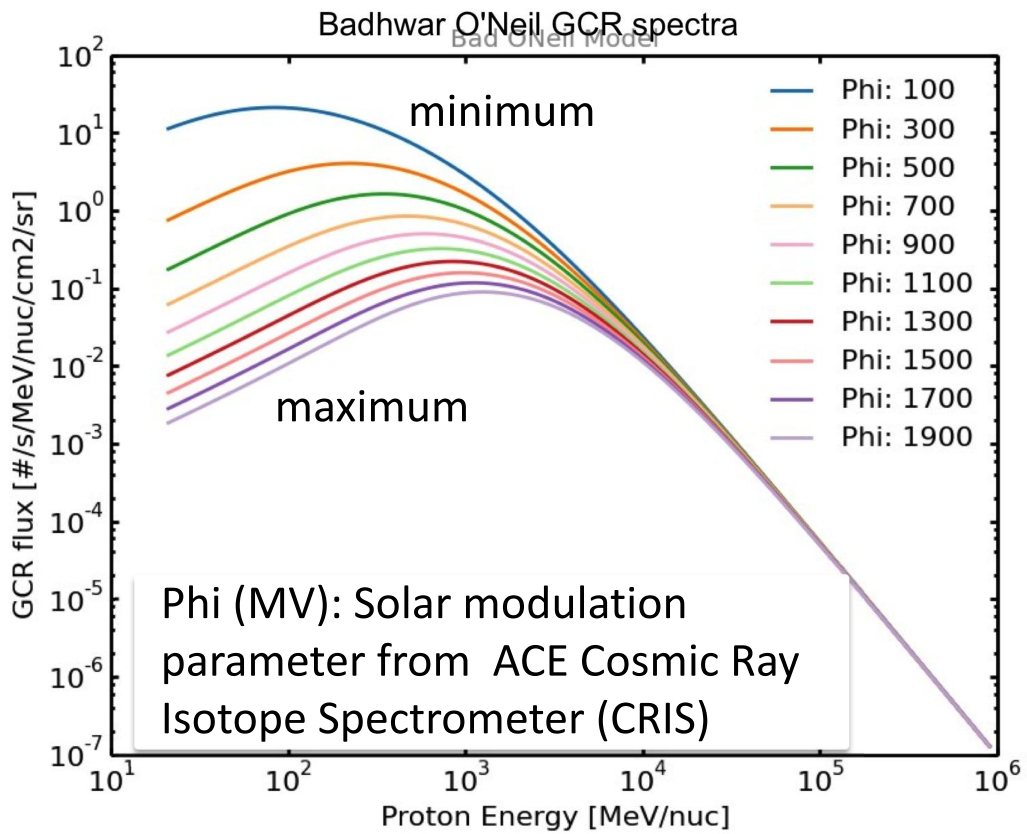

Forbush decrease

"Recurrent" FD: recur with the solar rotation period and are associated with corotating interaction regions （27-day variation)
"non- recurrent" FD: caused by the passage of transient solar wind structures (CME and its driven shock)

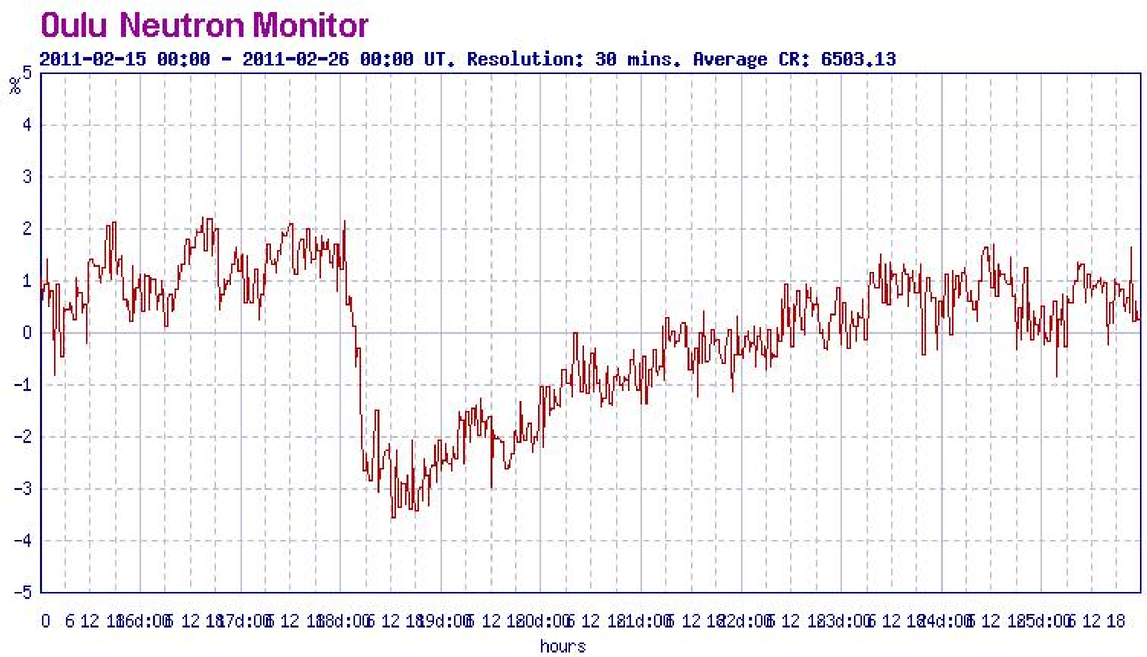

FD characteristics:

Rapid decrease of the GCR flux within a few hours to 1 or 2 days,
Gradual recovery in the coming a few days or 10 days

Two-step Forbush Decrease

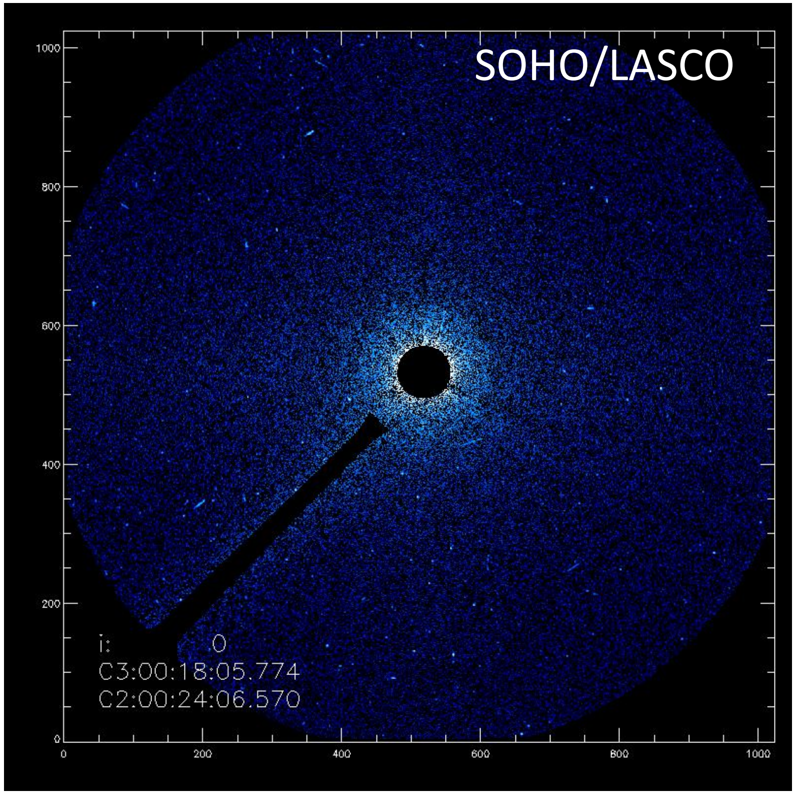

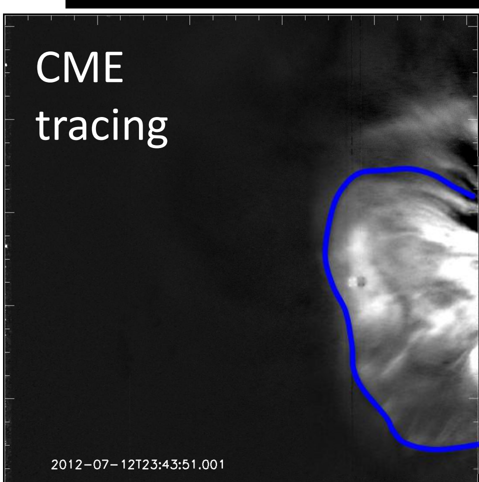

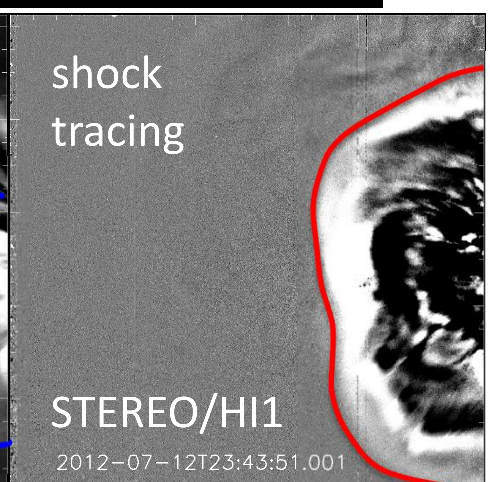

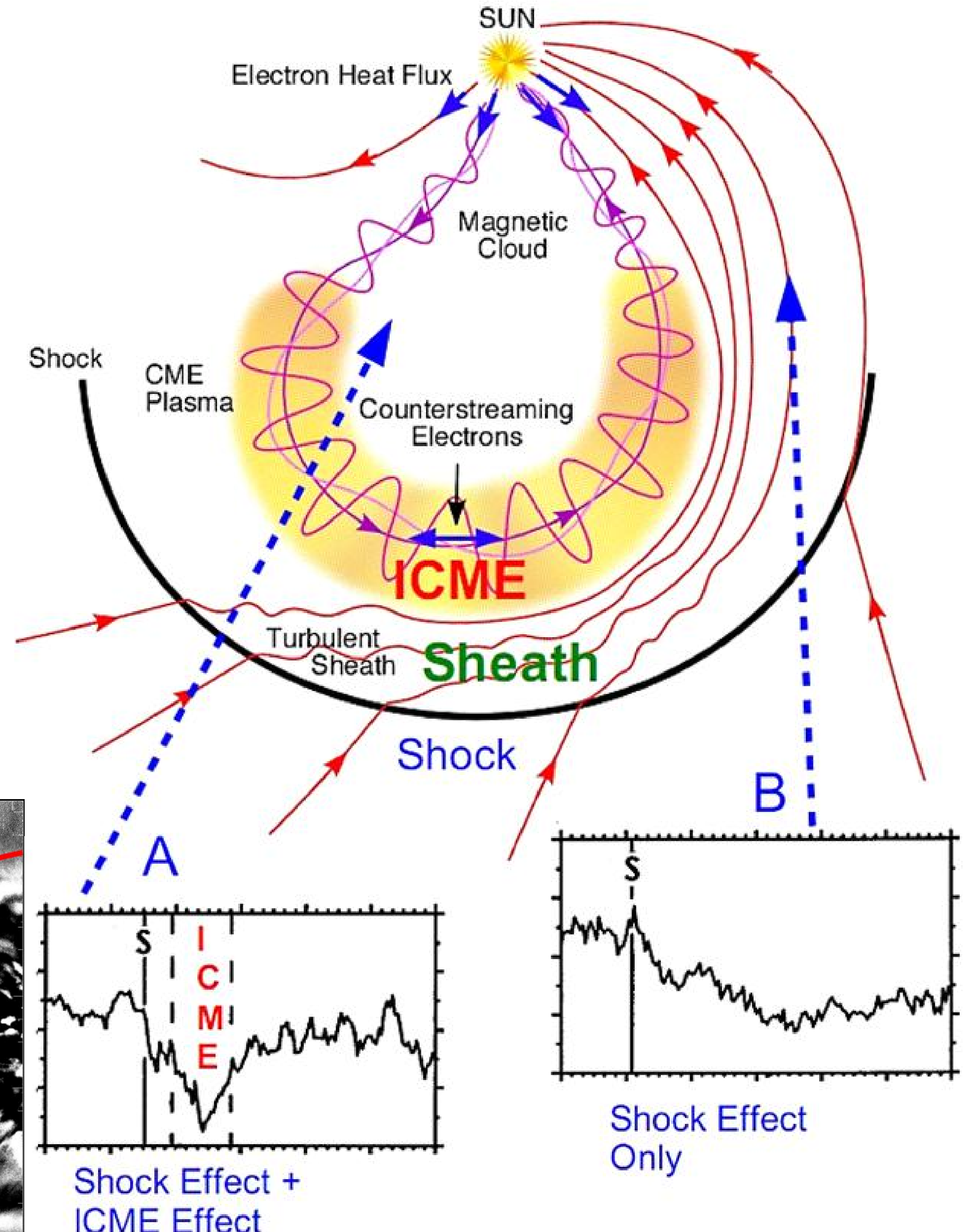

ICME propagation from 1 AU to 1.5AU

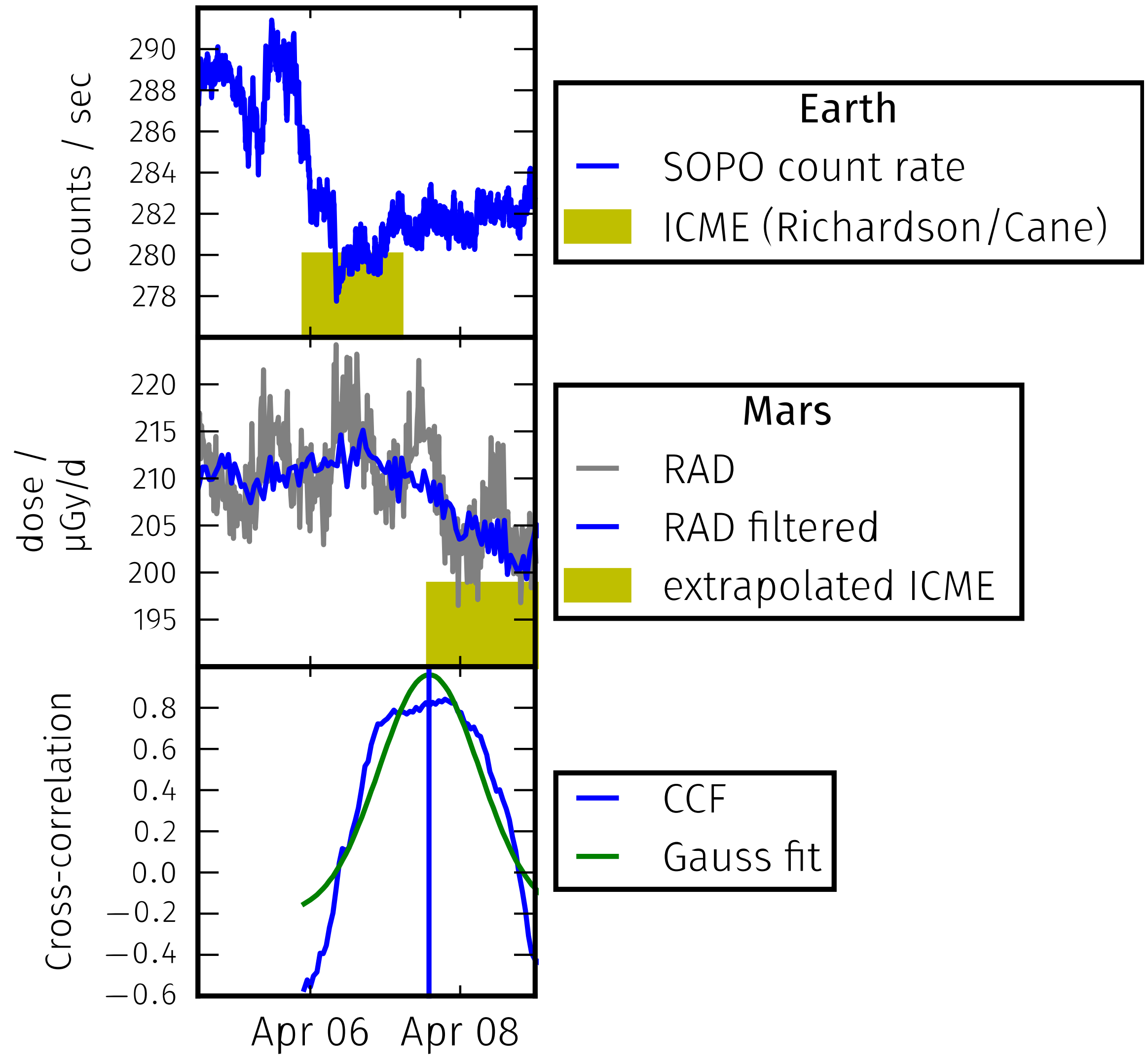

Von Forstner et al., 2017, in prep

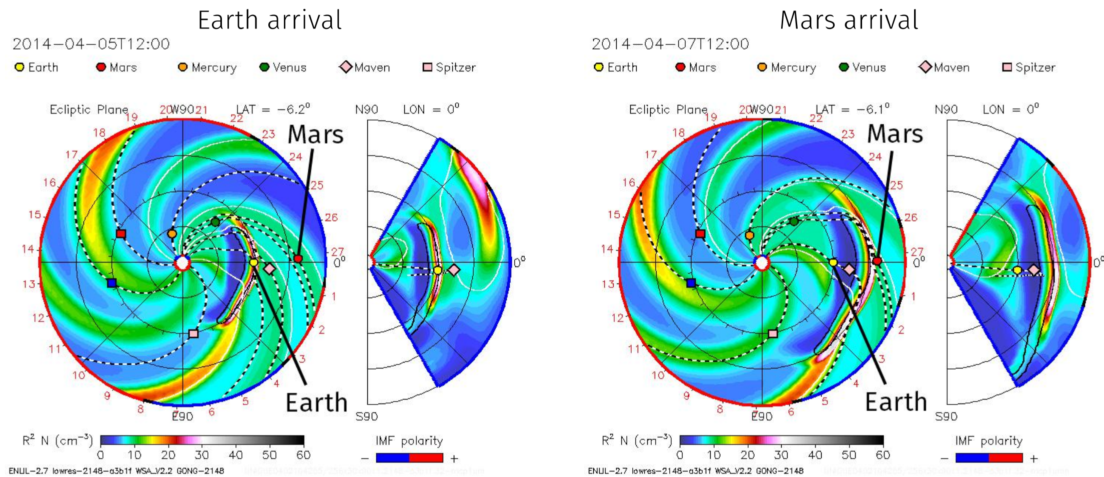

Earth arrival
2014−04−05T12:00
Earth
Mars
Mercury
Venus
Maven
Spitzer
Ecliptic Plane
LAT = −6.2°
LON = 0°
Mars
Earth
R² N (cm⁻³)
IMF polarity
ENLIL−2.7 lowres−2148−a3b1f WSA_V2.2 GONG−2148
Mars arrival
2014−04−07T12:00
LAT = −6.1°

6

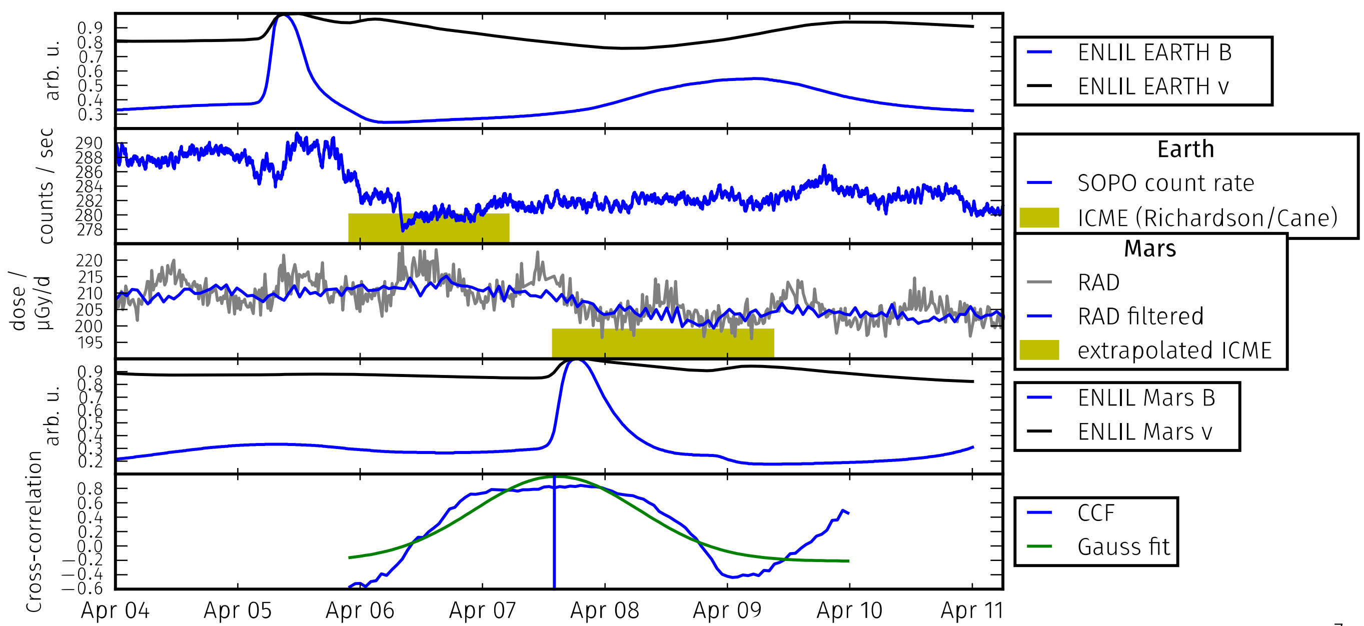

ENLIL EARTH B
ENLIL EARTH v
Earth
SOPO count rate
ICME (Richardson/Cane)
Mars
RAD
RAD filtered
extrapolated ICME
ENLIL Mars B
ENLIL Mars v
CCF
Gauss fit
arb. u.
counts / sec
dose / µGy/d
Cross-correlation
Apr 04
Apr 05
Apr 06
Apr 07
Apr 08
Apr 09
Apr 10
Apr 11

FD for different CME events

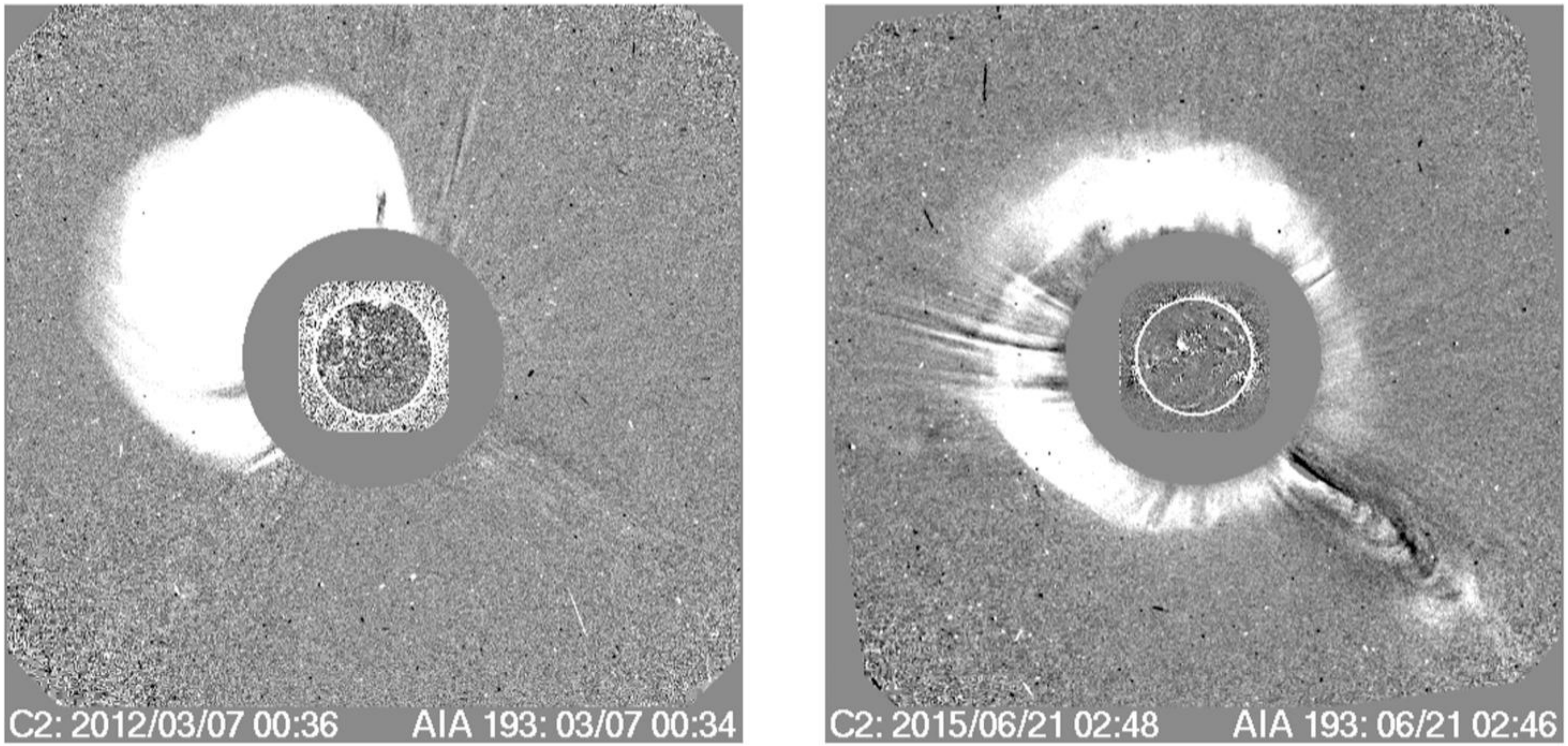

Figure 1. LASCO C2 images of the CMEs on 2012 March 7 at 00:36 UT (left) and 2015 June 21 at 02:48 UT (right).

Zhao et al. 2016

Key parameters of FD : amplitude,recovery time as a function of median energy

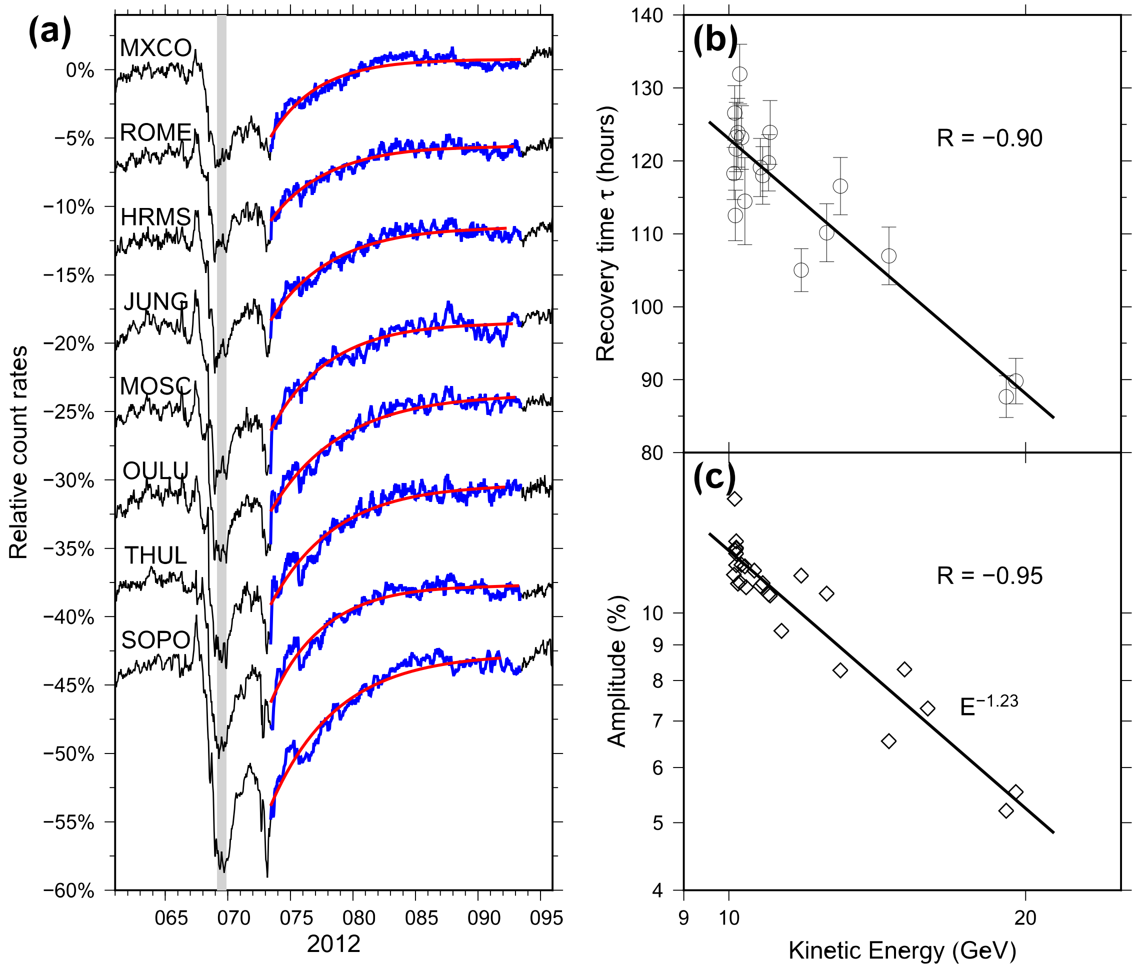

Recovery time:

$$\delta I = \frac{I_0 - I}{I_0} = A \cdot \exp\left(-\frac{t - t_0}{\tau}\right)$$

Median energy:

$$E_m = 0.0877P_c^2 + 0.154P_c + 10.12$$

2012-Mar-07 event

LHAASO: extend the FD study to higher energies

2012-Mar-07

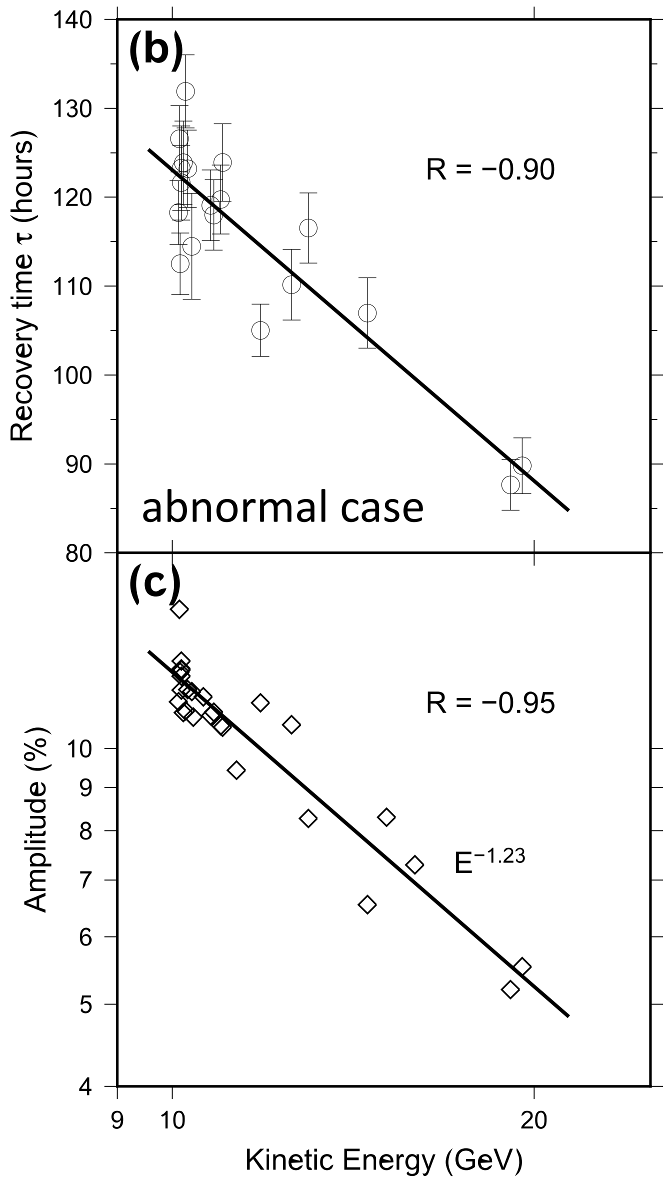

2015-June-21

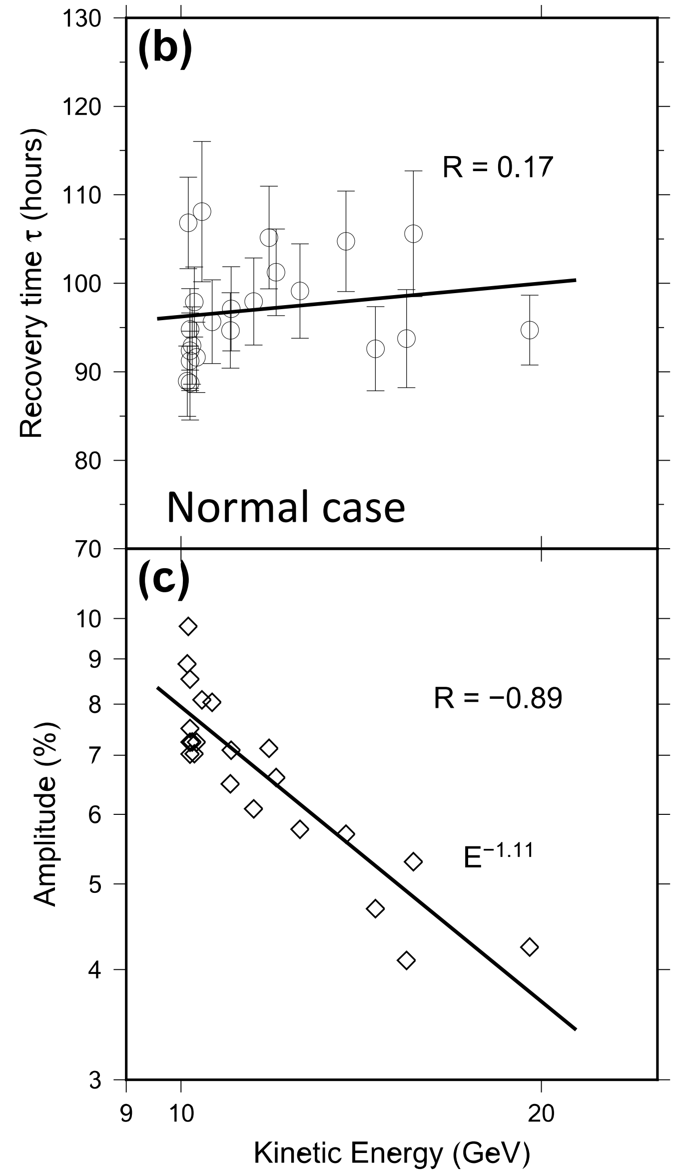

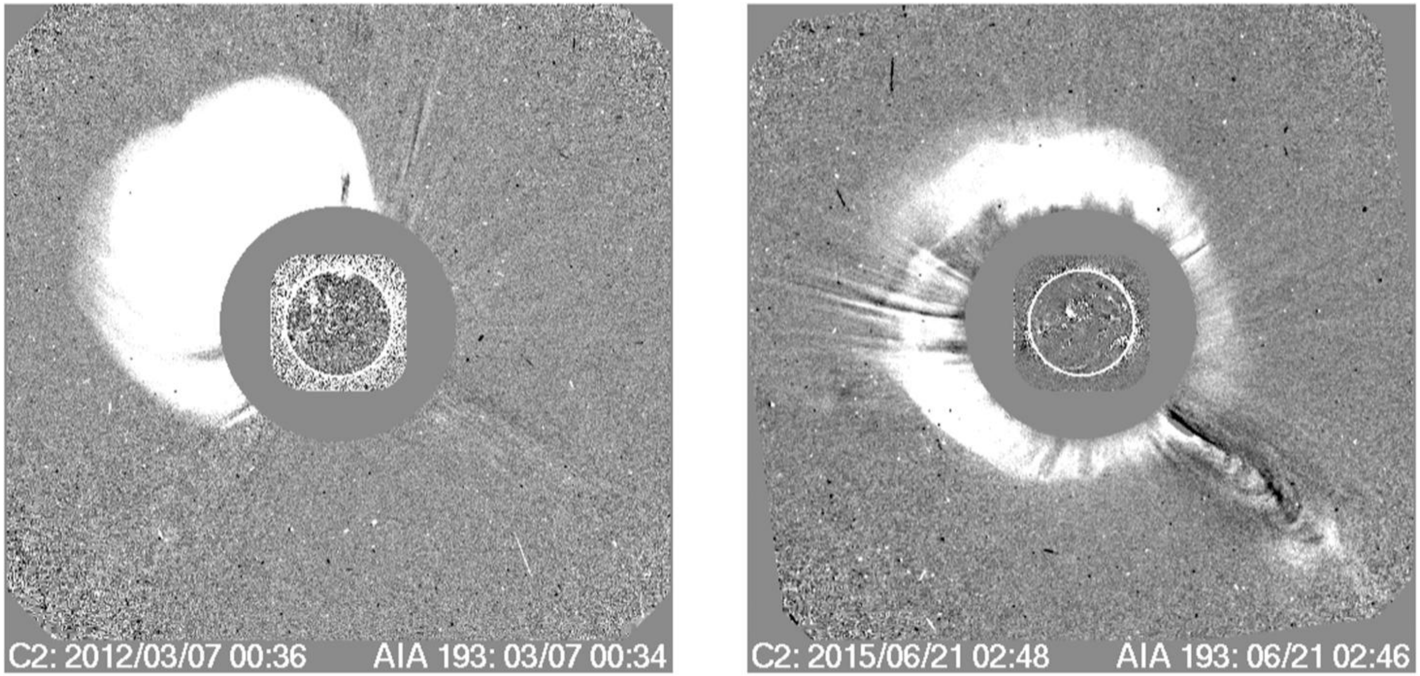

Figure 1. LASCO C2 images of the CMEs on 2012 March 7 at 00:36 UT (left) and 2015 June 21 at 02:48 UT (right).

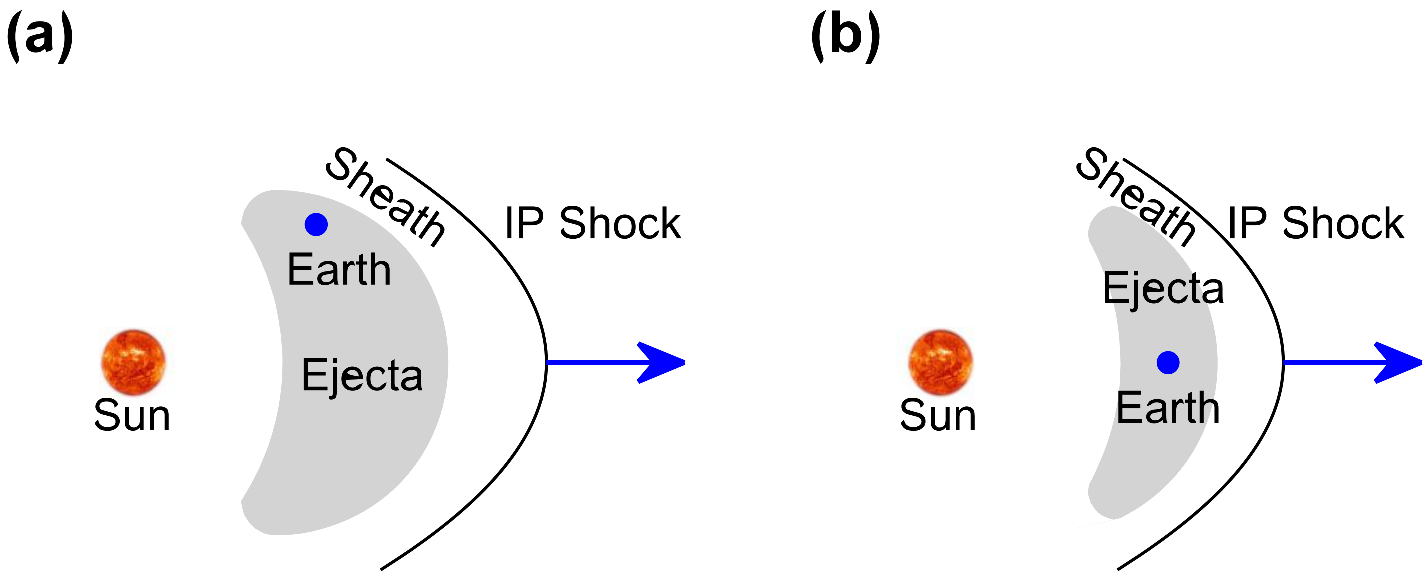

Figure 9. Schematic diagram (not to scale) explaining (a) Event 1 and (b) Event 2.

2012-Mar-07 event
Projections of the propagation of the 3D shock on the solar equatorial plane

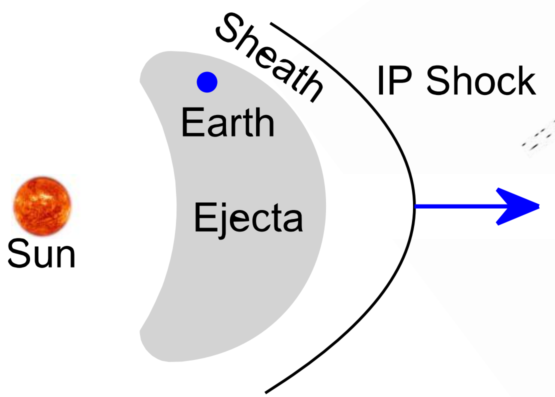

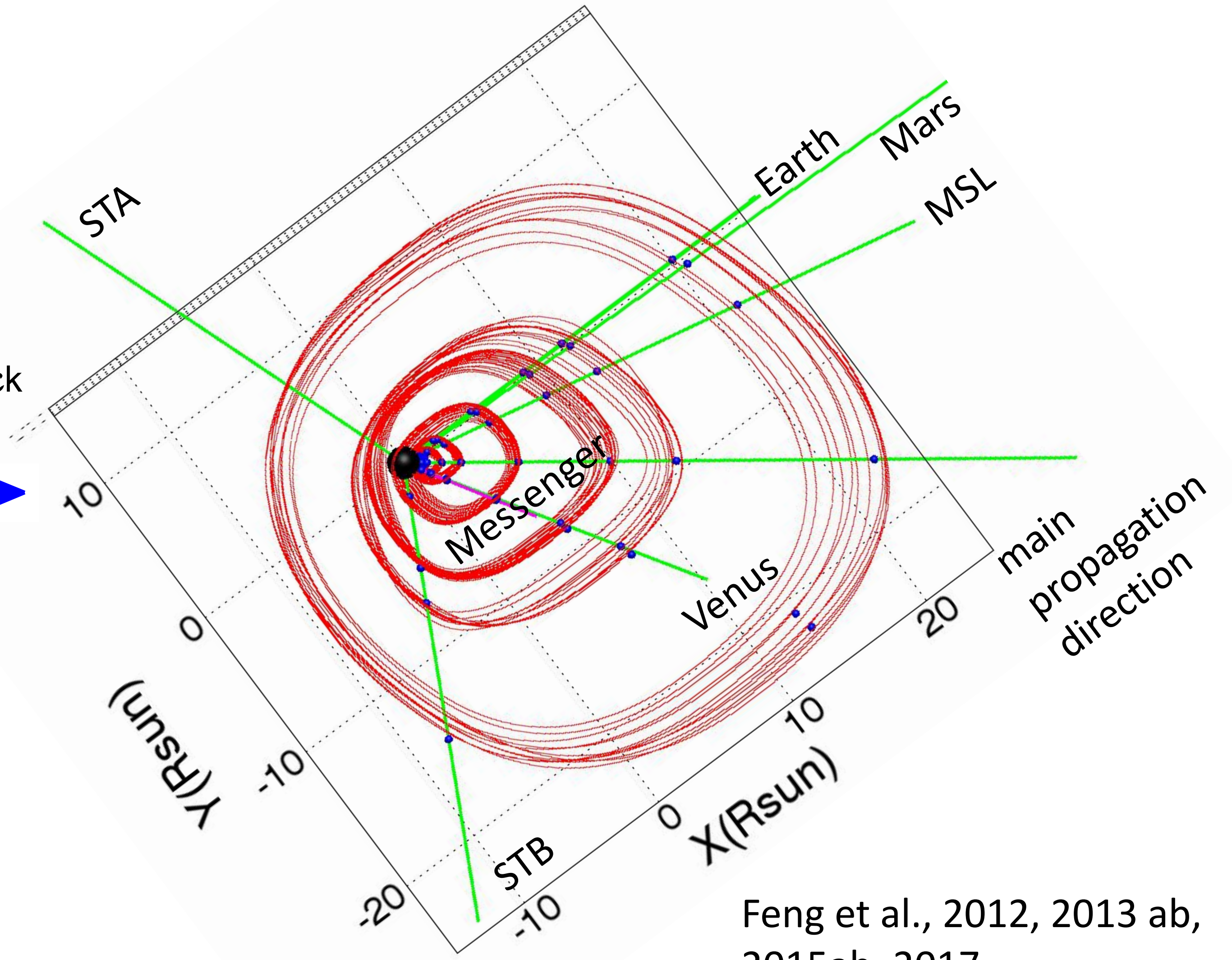

Feng et al., 2012, 2013 ab, 2015ab, 2017

1D Simulation of FD

$$\frac{\partial f}{\partial t} + V_{sw} \bullet \nabla f - \nabla \bullet \left(\kappa \bullet \nabla f \right) - \frac{1}{3} \nabla \bullet V_{sw} \frac{\partial f}{\partial \ln P} = 0$$

convection | diffusion | Energy change

1D case

$$\frac{\partial f}{\partial t} = \kappa_{rr} \frac{\partial^2 f}{\partial r^2} + \left[\frac{\partial \left(r^2 \kappa_{rr} \right)}{r^2 \partial r} - V_{sw} \right] \frac{\partial f}{\partial r} + \frac{\partial \left(r^2 V_{sw} \right)}{3 r^2 \partial r} \frac{\partial f}{\partial \ln P}$$

Diffusion coefficient and its scale μ

$$\kappa_{rr}(t,r) = \frac{\kappa_M + \kappa_m}{2} + \frac{\kappa_M - \kappa_m}{2} \bullet \cos\left(2\pi \frac{t - r / V_{sw}}{\boldsymbol{T}} \right)$$

$$\kappa'_{rr}(t,r) = \mu \bullet \kappa_{rr}(t,r)$$

[Li et al.,2008]

Ni et al., 2017, in prep

1D Simulation of FD

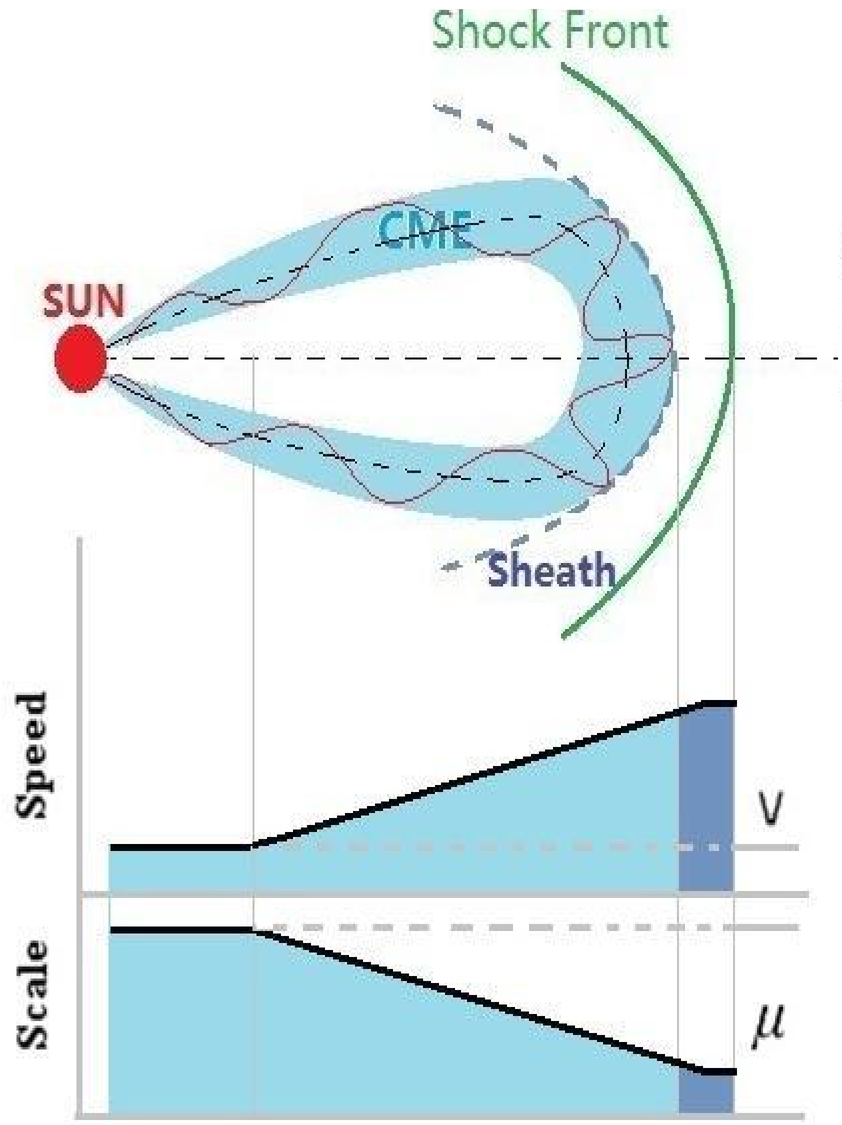

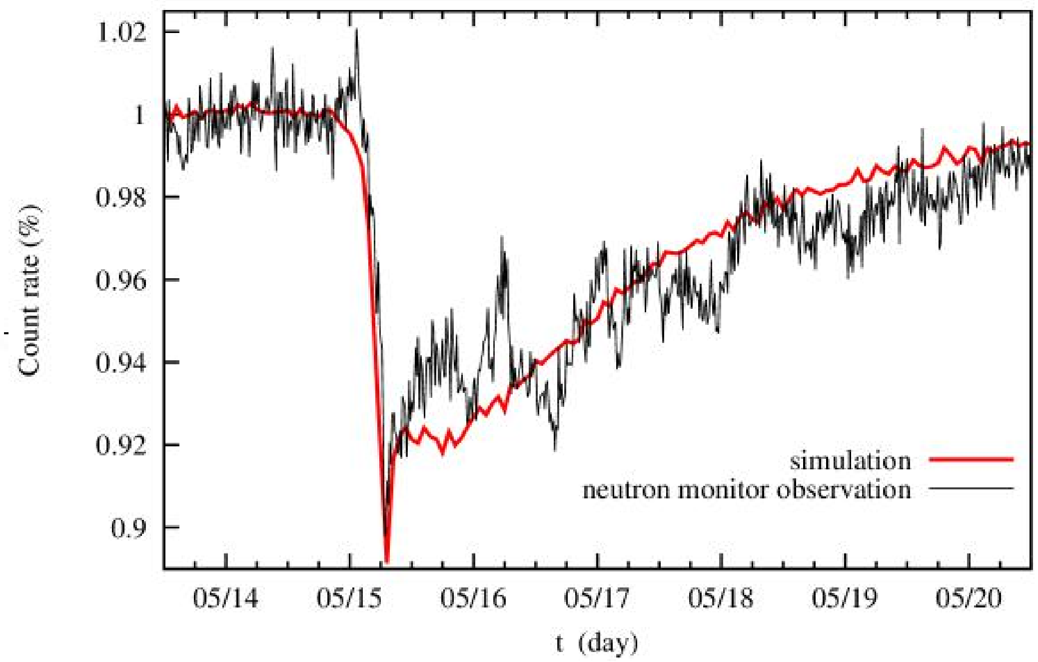

μ is inversely proportional to V

FD prediction- shock precursor

Decrease of cosmic ray intensity in front the shock; have nearly the same rigidity spectrum as the FD.

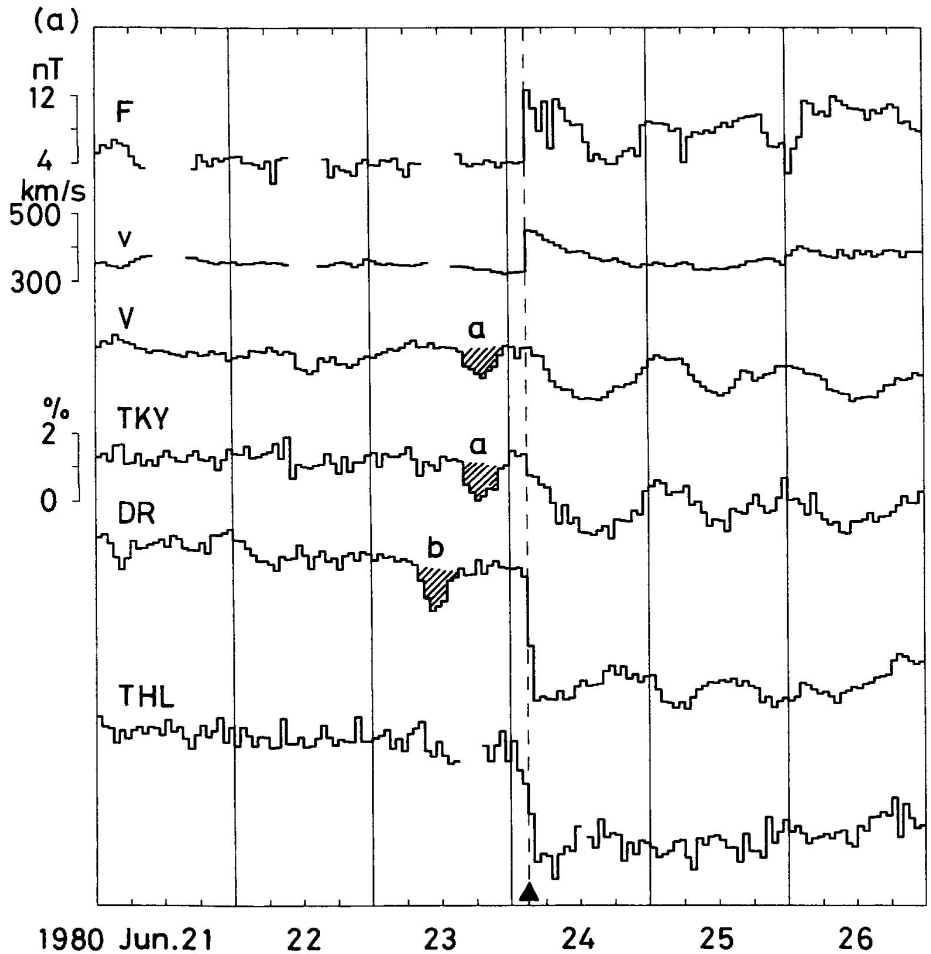

Nagashima et al. 1992

Decrease of cosmic ray intensity in front the shock- shock precursor

Z=0: oblique shock front position
Z>0: shock upstream
Z<0: shock downstream (region of FD)

Loss cone or deficit cone: particles comes from the shock downstream

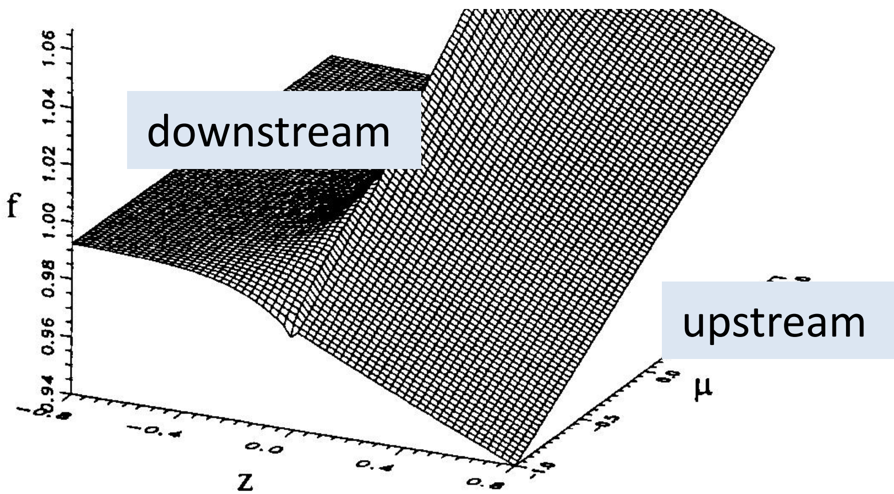

Particle distribution as a function of distance to shock front and pitch angle

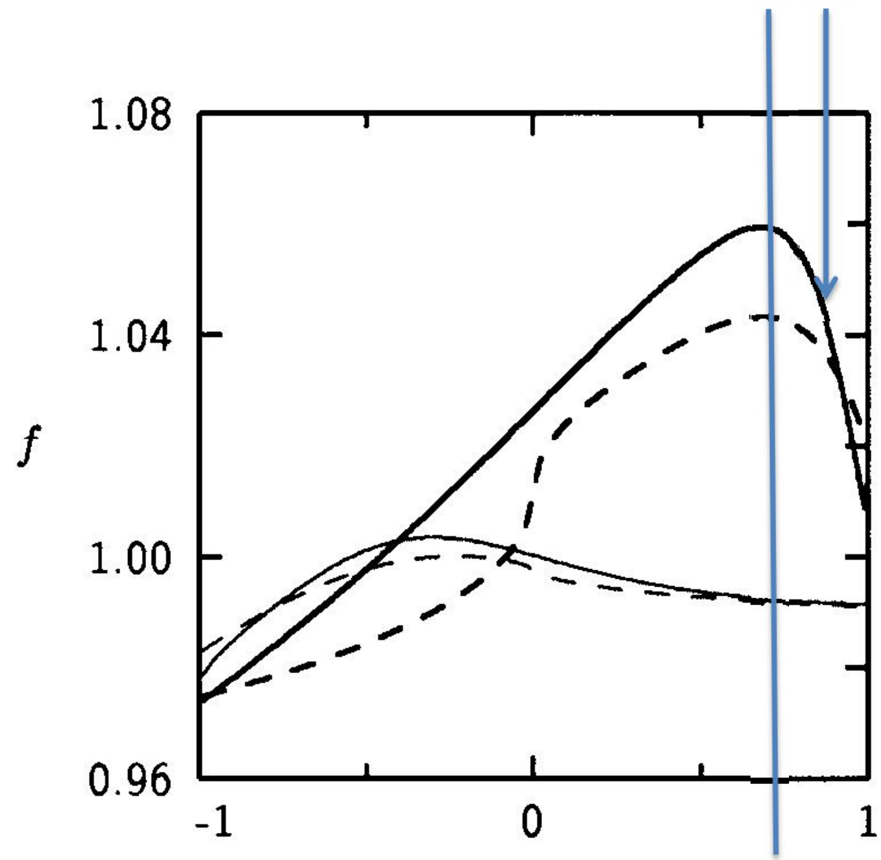

μ Ruffolo 1999

Shock prediction

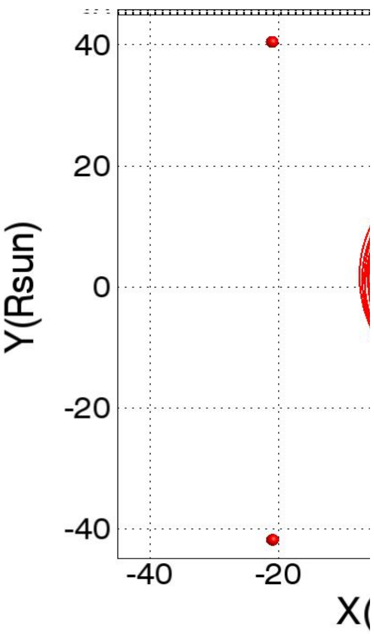

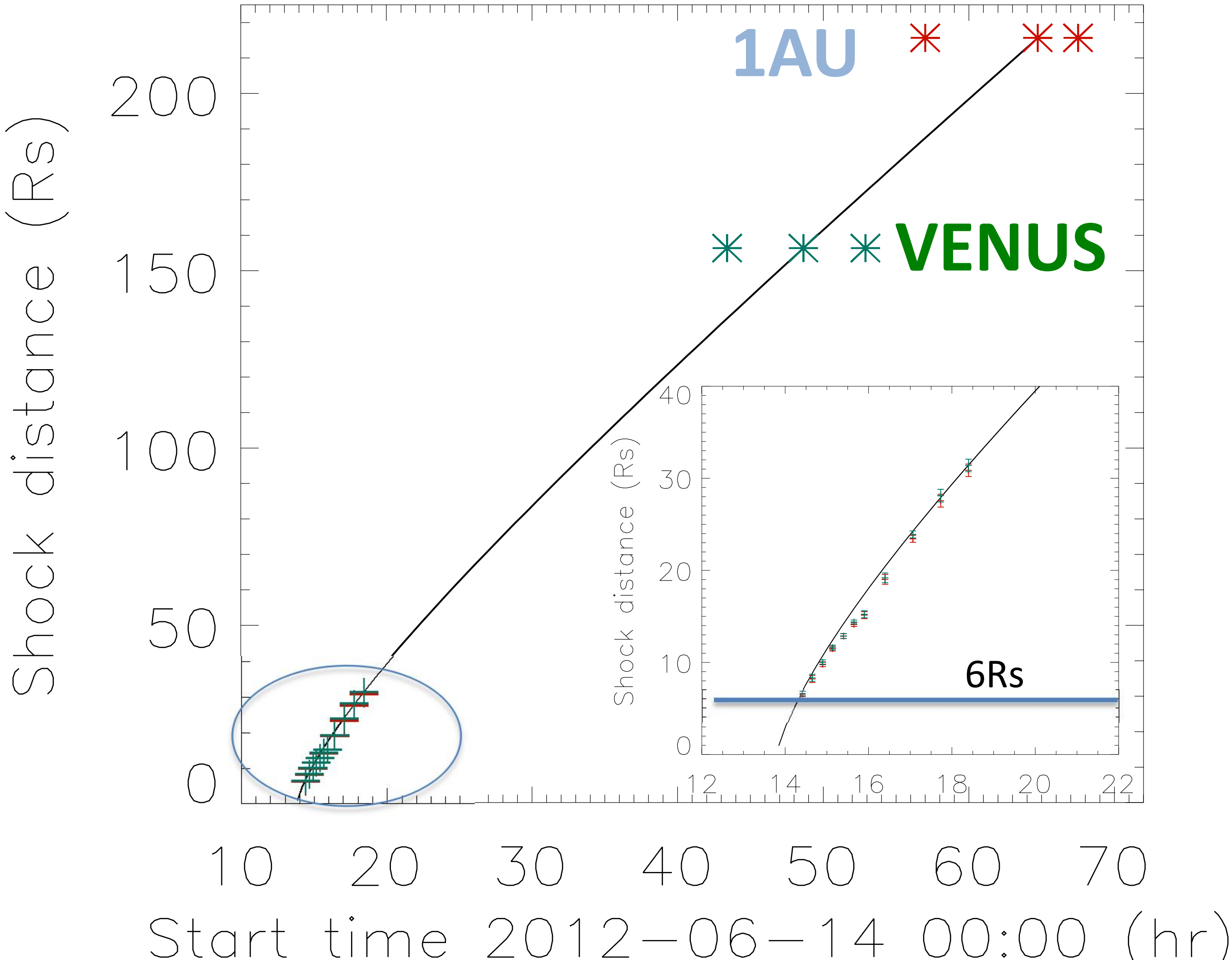

Shock Prop
Model the
after the sh
a maximum
wave scena

Feng et al. 2017, in prep

More work to be done …

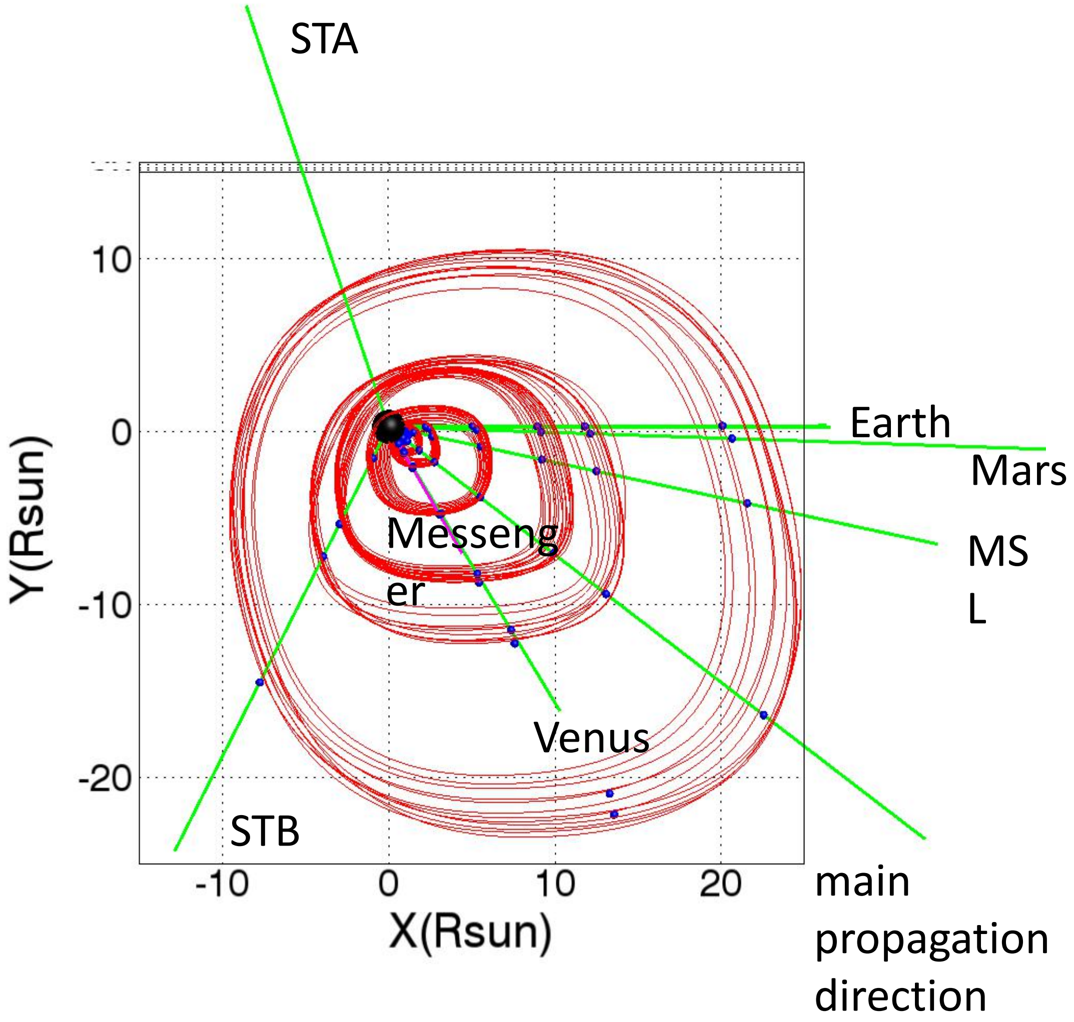

1. Simulations along the CME/shock flank
2. Compare the simulations with the cosmic ray flux at Earth, Mars, etc.

More work to be done …

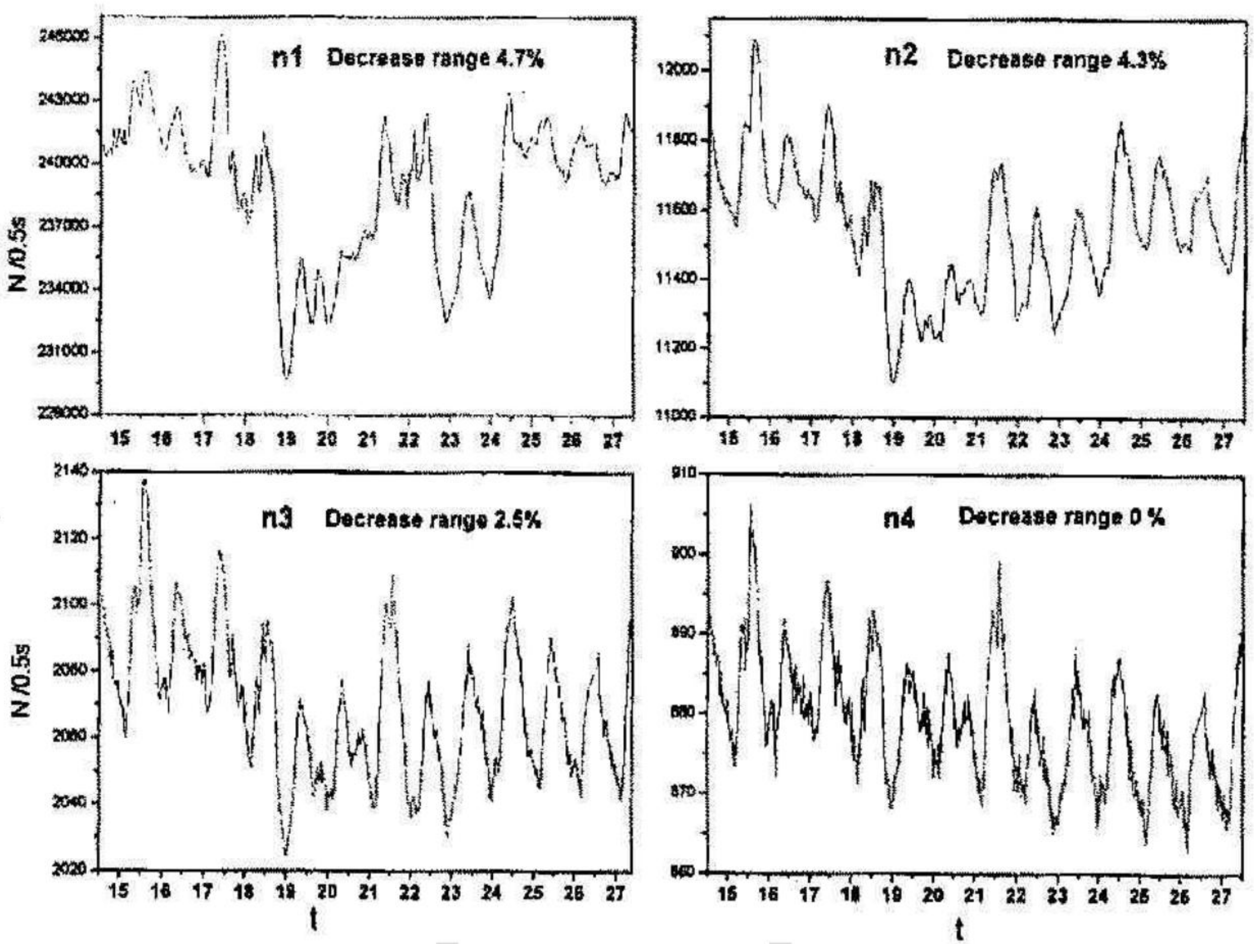

Jia et al., 2005

ARGO-SPT experiment: FD in different energy ranges

1. More events study

1. Simulations of FD in different energy ranges

Sun shadow and CME shadow

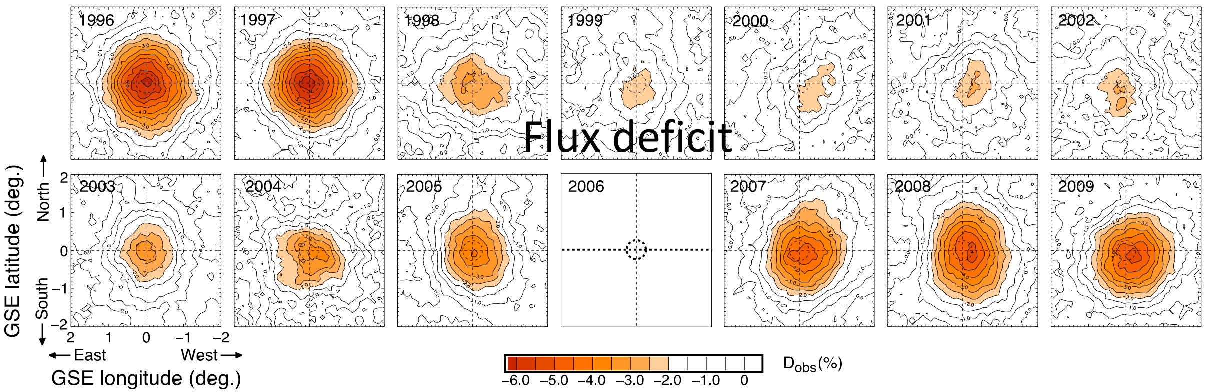

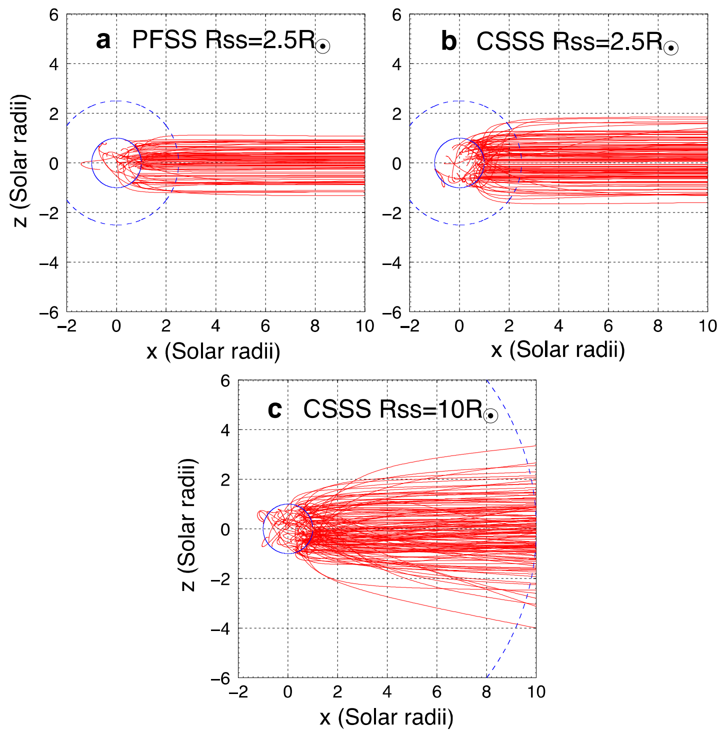

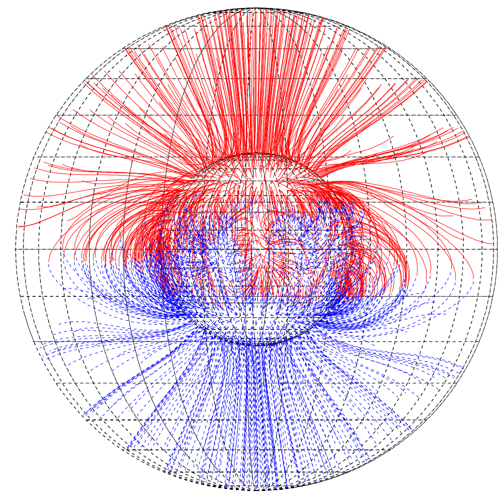

a
PFSS

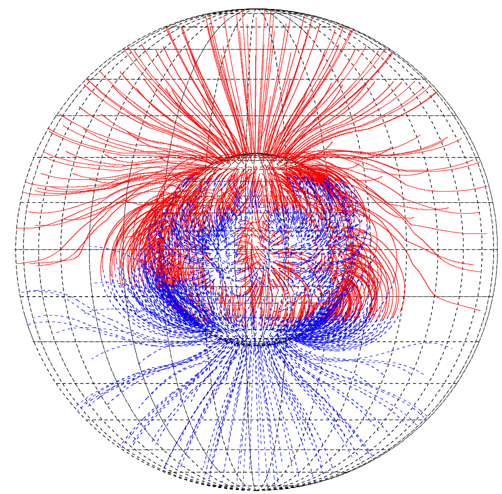

b
CSSS

Amenomori et al., 2013

Coronal magnetic field model

Extrapolation from line of sight magnetic field

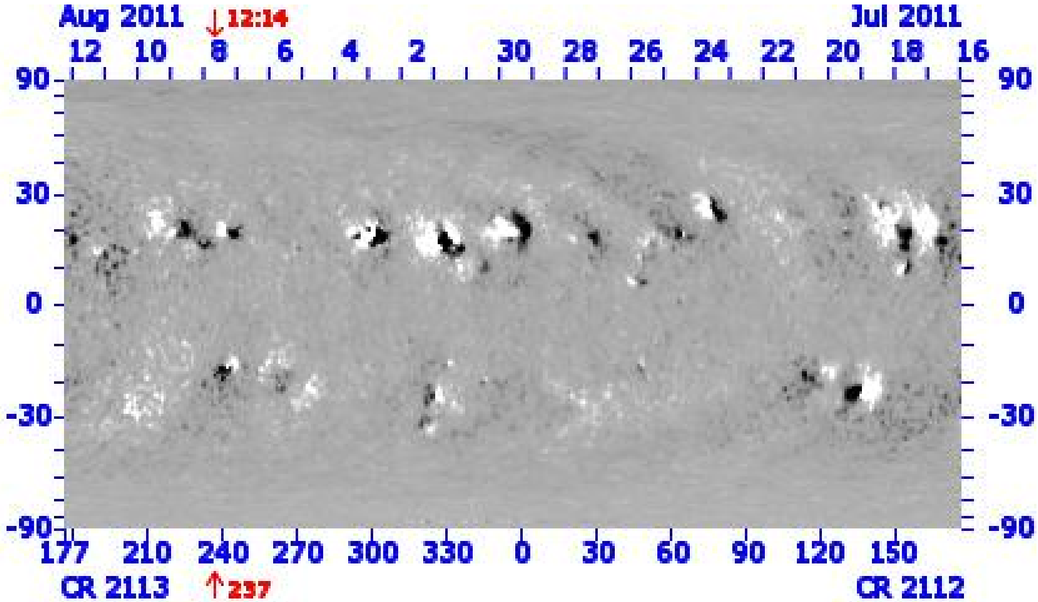

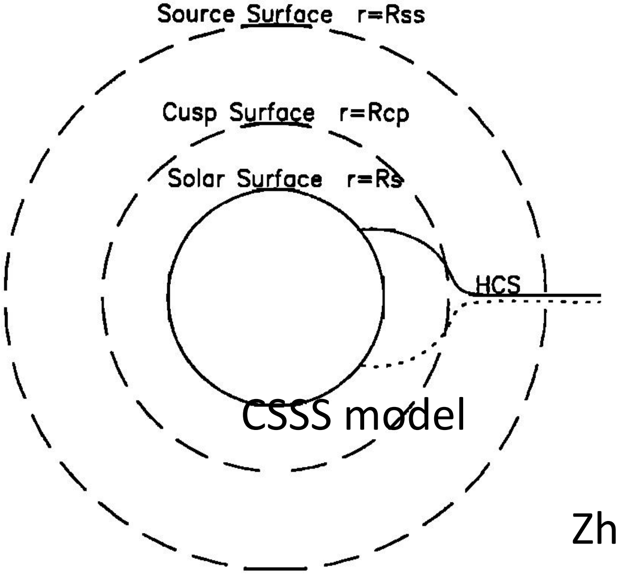

Zhao et al. 1995

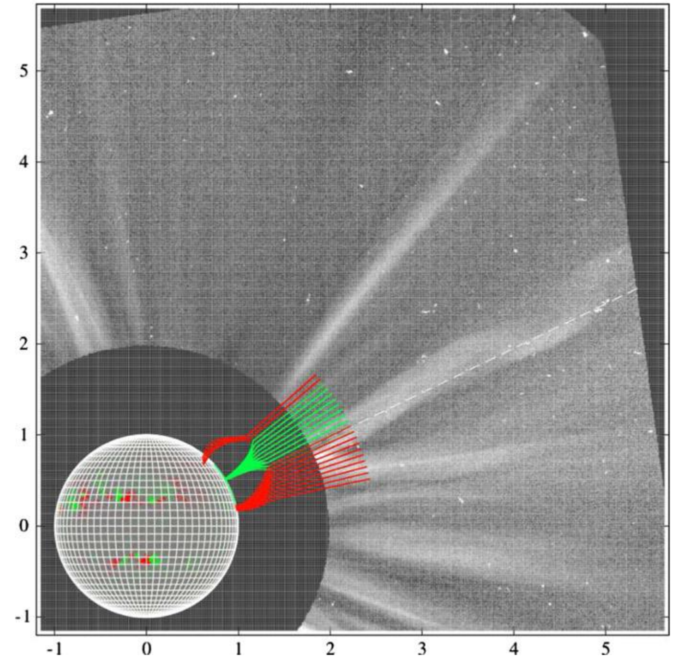

Linear force free field extrapolation

$$\mathbf{B} \cdot \nabla \alpha = 0,$$

$$\nabla \times \mathbf{B} = \alpha \mathbf{B}.$$

Feng et al. 2013c

Coronal magnetic field model

Extrapolation from vector magnetic field

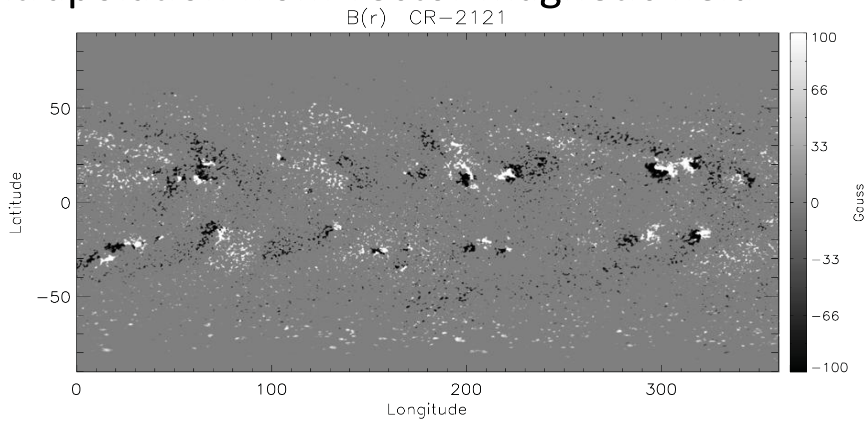

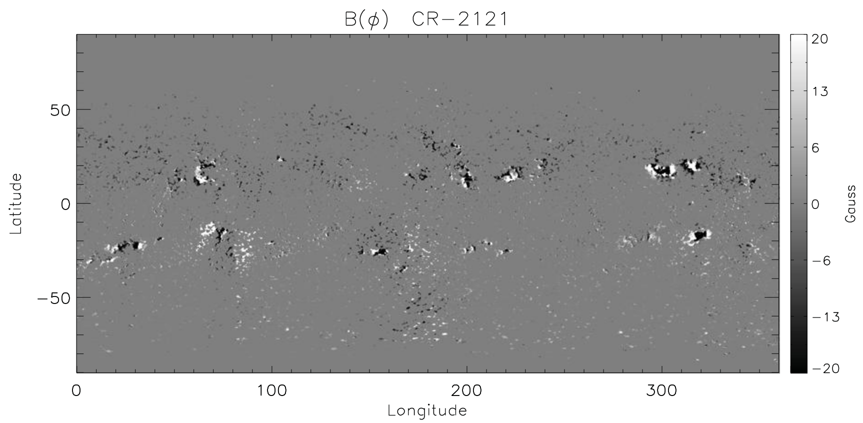

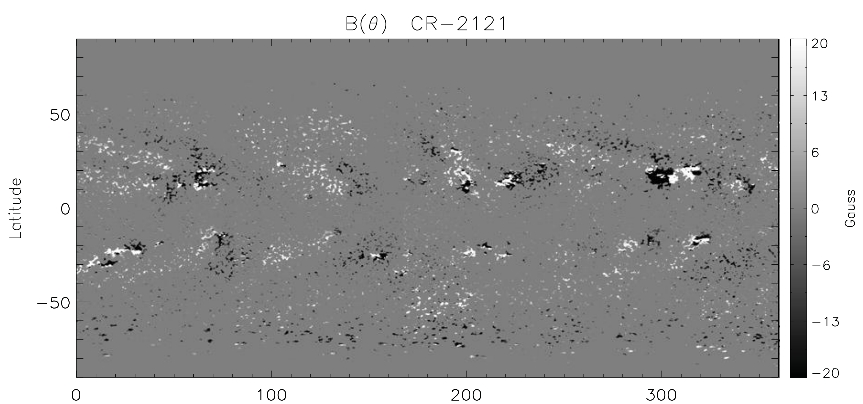

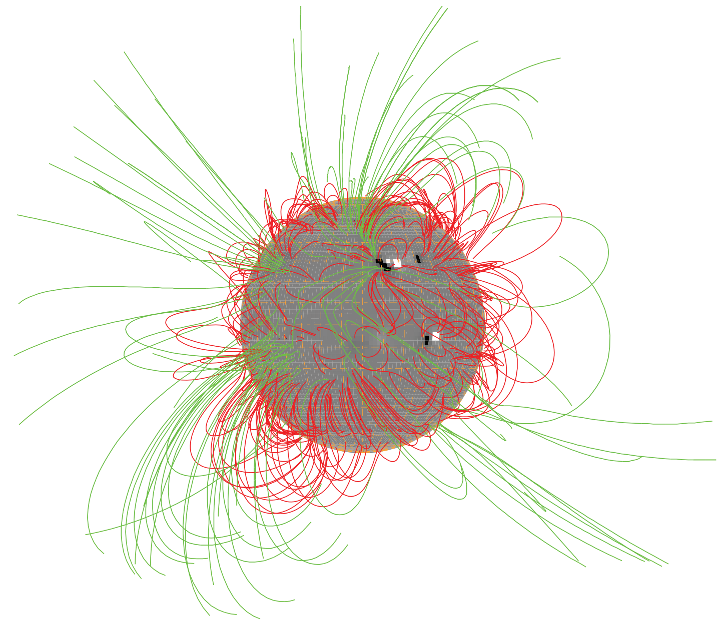

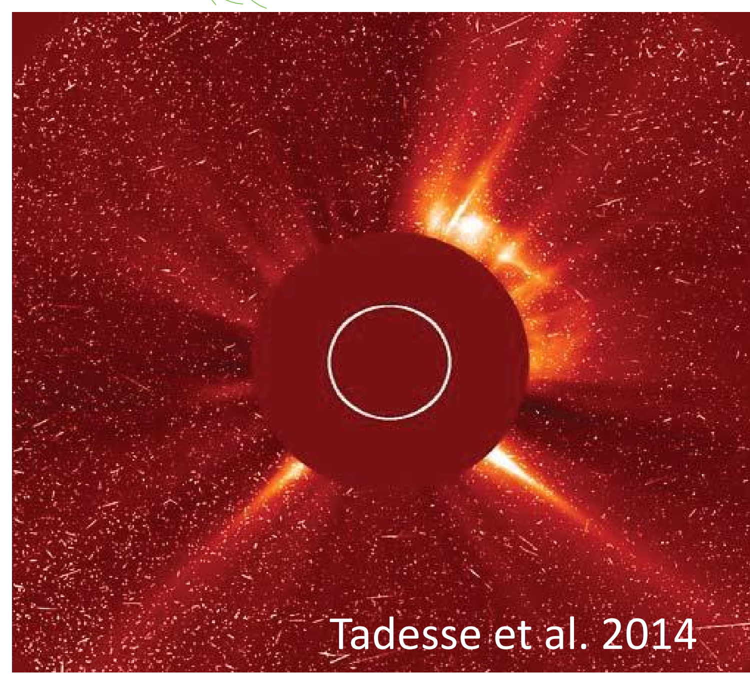

MHD simulations of interplanetary magnetic field

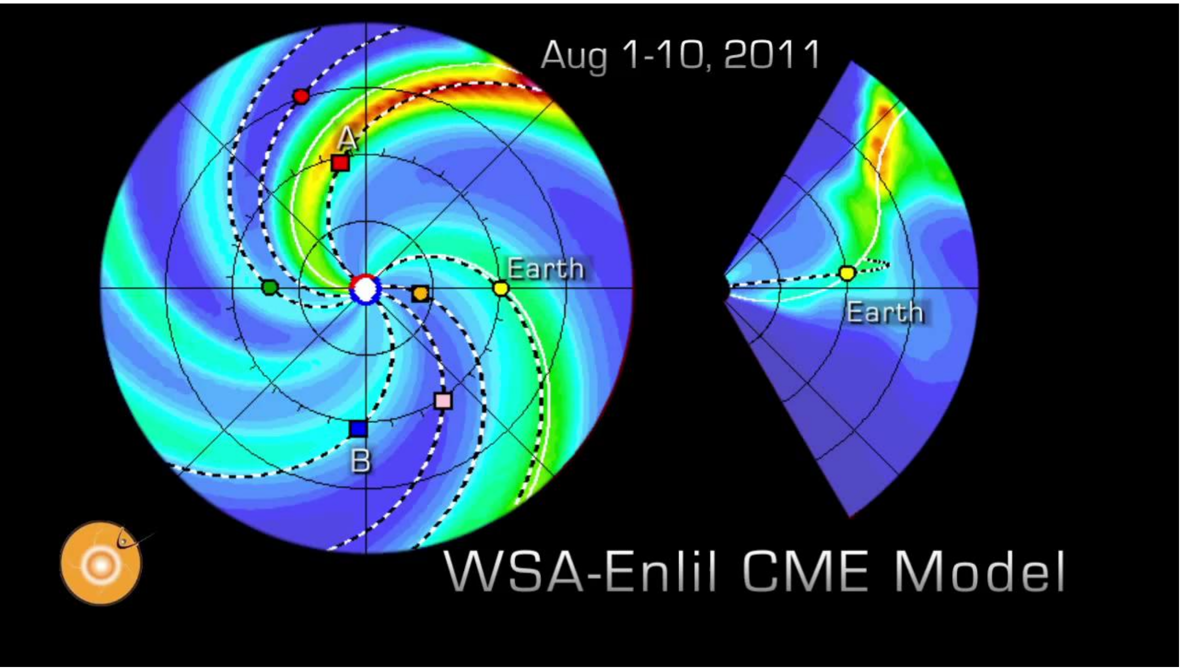

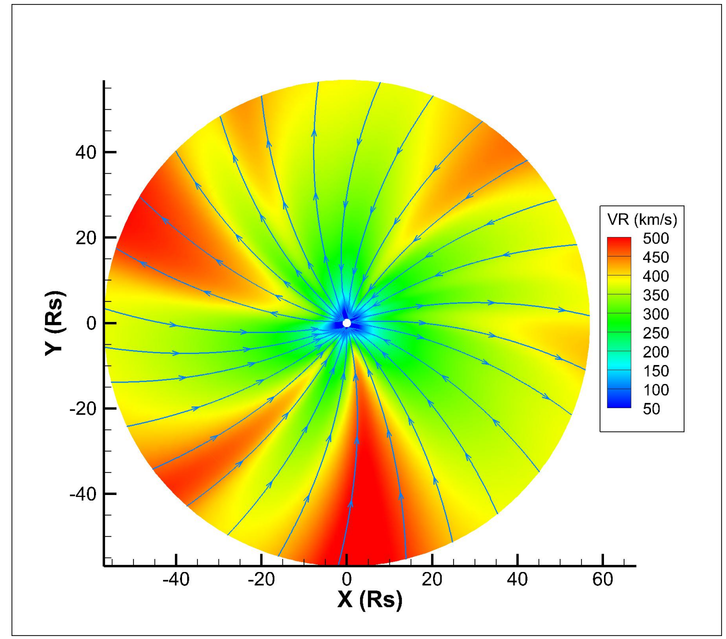

NSSC COIN-TVD model :
Shen et al., 2013
Feng et al., 2017, in prep

CME shadow

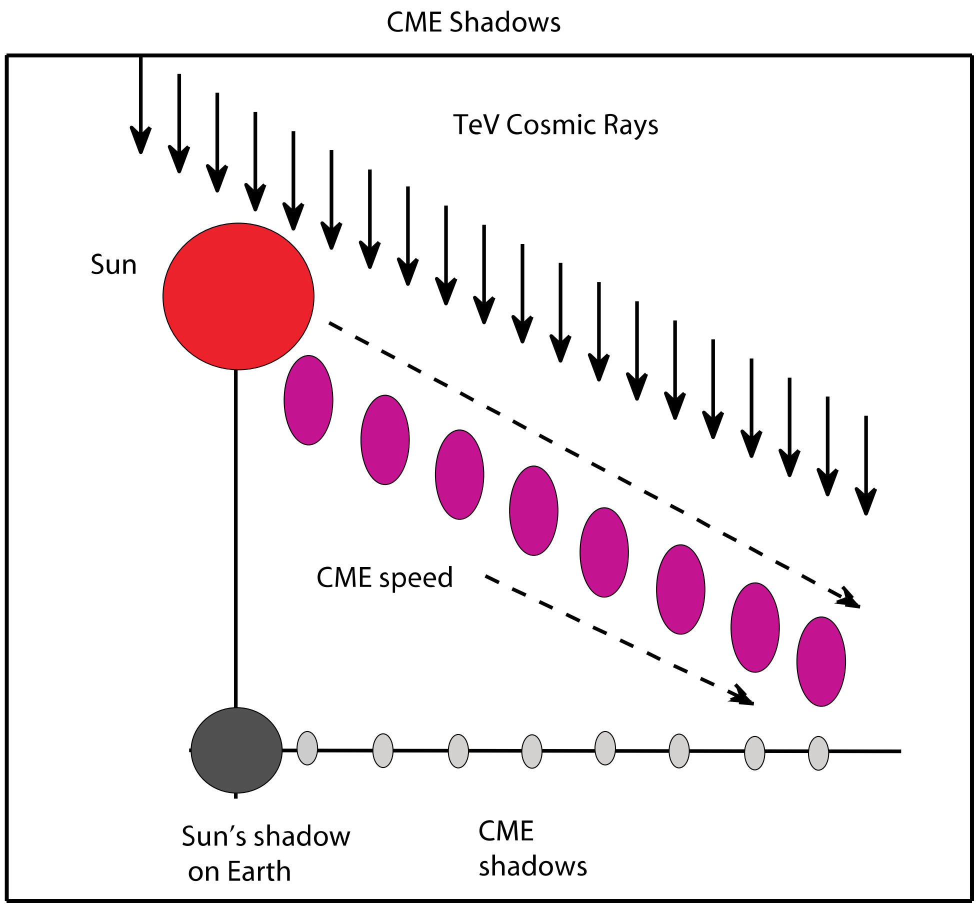

LHAASO science document

MHD simulations of CME propagation

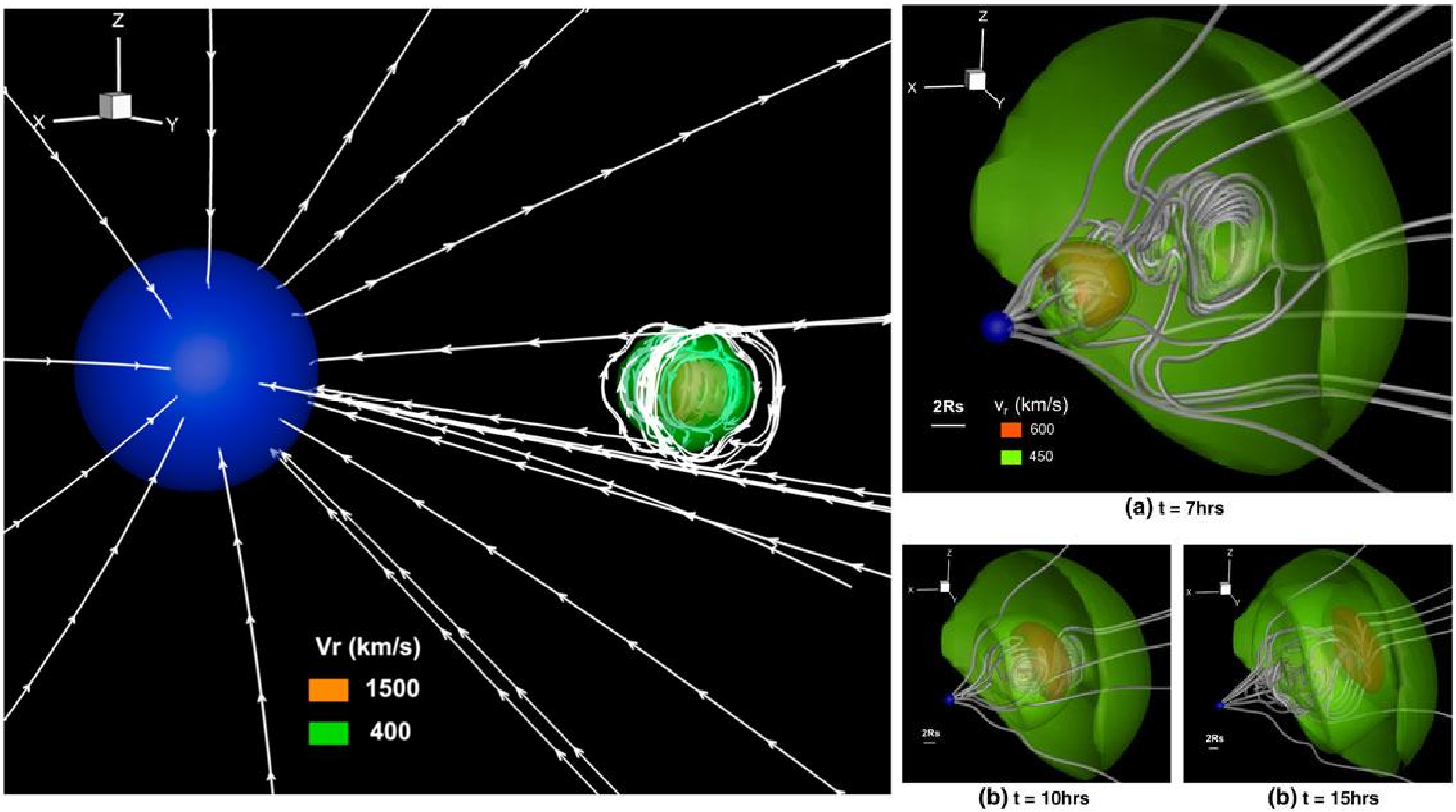

Shen et al., 2013, 2014

宇宙线传输

- Heliospheric transport of GCR is described by Parker's theory (Parker, 1965; Toptygin, 1985)

Four basic processes：

- the diffusion of particles due to their scattering on magnetic inhomogeneities,
- the convection of particles by out-blowing solar wind,
- adiabatic energy losses in expanding solar wind,
- drifts of particles in the magnetic field, including the gradient-curvature drift in the regular heliospheric magnetic field, and the drift along the heliospheric current sheet, which is a thin magnetic interface between the two heliomagnetic hemispheres.

宇宙线的调制

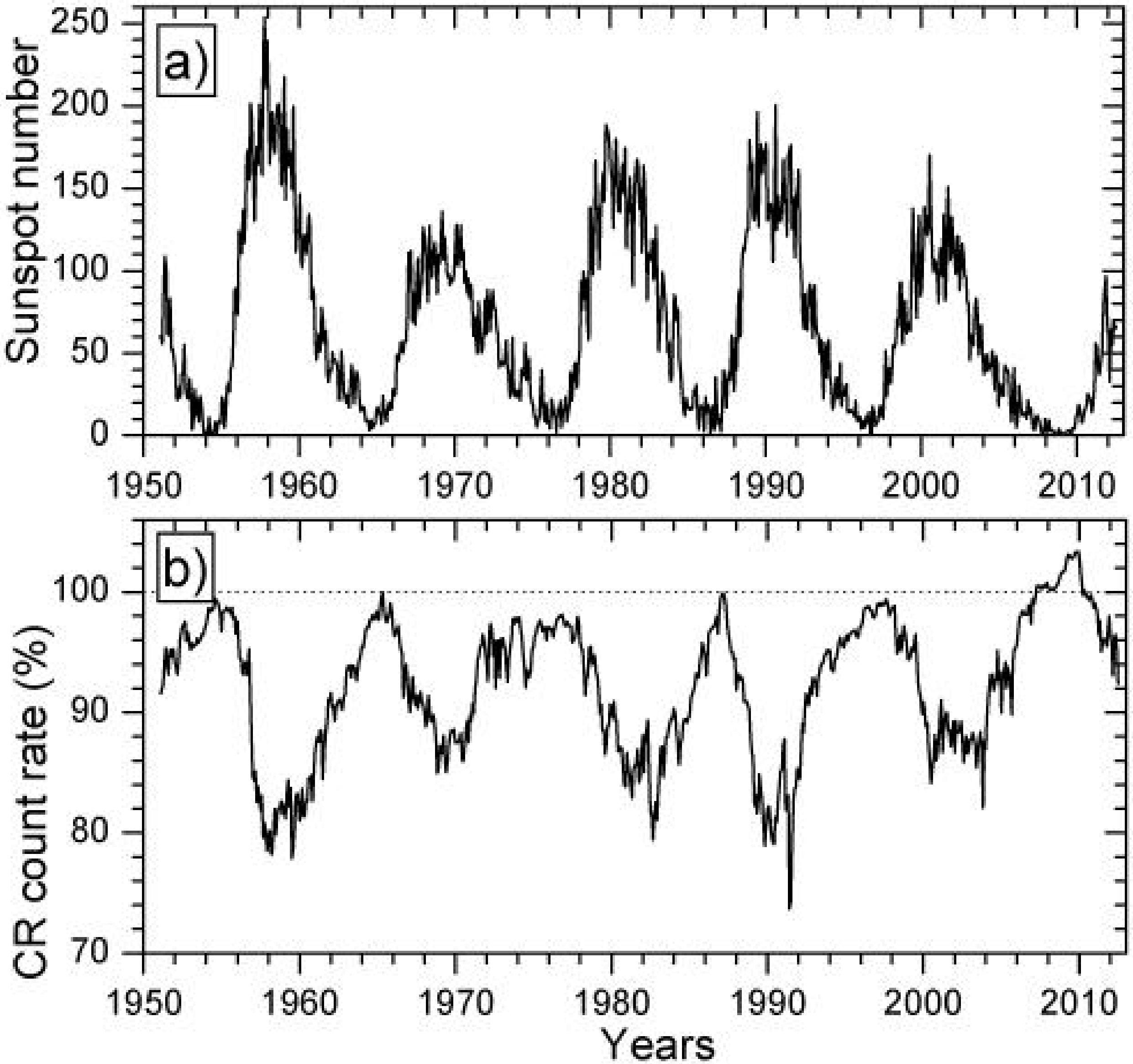

11 year cycle: solar activity
22 year cycle:
Sharp and flat maxima.

the increase of CR flux in 2009, when it was the highest ever recorded by NMs as caused by the favorable heliospheric conditions (unusually weak heliospheric magnetic field and the flat heliospheric current sheet) (McDonald *et al.*, 2010).

Usoskin et al., LRSP